Pergamon

0301-9322(94)00074-3

Int. J. Multiphase Flow Vol. 21, No. 2, pp. 285–303, 1995

0301-9322/95 $9.50 + 0.00

SEDIMENTATION OF A CYLINDRICAL PARTICLE IN AN OSCILLATING FLUID

M. MALEKI-ARDEBILI

Lehrstuhl für Mech. Verfahrenstechnik und Strömungsmechanik der Universität Kaiserslautern, Erwin-Schrödinger Str., Postfach 3049, 6750 Kaiserslautern, Germany

(Received 30 January 1994; in revised form 11 October 1994)

Abstract—The free motion of a single cylindrical particle in an incompressible sinusoidally horizontally and vertically oscillating flow field under consideration of the gravity field is investigated. A new numerical method based on the overlapping grid approach is developed. The influence of Reynolds number and density ratio on the particle motion is also discussed.

Key Words: numerical simulation, overlapping grid, free particle motion, particle–fluid interaction

INTRODUCTION

The unsteady motion of solid particles in an unstationary flow field is of great interest in many engineering applications. The forces acting on the particles have either quasistationary (e.g. the gravity force on a particle in a fluid at rest) or time-dependent origin (e.g. the motion of particles in a turbulent flow field). Small particles moving in a turbulent flow field are embedded in turbulent eddies (characteristic length of the particle < length of the turbulent eddy). In this case the particle inflow is irregular in all directions. Due to the complexity of the above-mentioned problem, the particle motion in a sinusoidally oscillatory flow field will be numerically investigated. Previous experimental and theoretical works are restricted to vertical oscillations (oscillations parallel to the settling direction) of spherical particles. The motion of non-spherical particles plays an important role in many branches of science such as aerosol physics, rheology, biology and atmospheric science. In the present work the motion of a cylindrical fiber-like particle (particle diameter $\ll$ particle length) in a vertically and horizontally (perpendicular to the settling direction) oscillating flow field will be examined. Several researchers have found that: larger fibres, with Re_p greater than about 0.01, will settle with their major axis oriented perpendicularly to the direction of motion. With increasing Re_p, longer fibres are still stable in the perpendicular orientation (see Willeke *et al.* 1992).

Experimental works on spherical particles were carried out, for example, by Schoeneborn (1975), Odar & Hamilton (1964), Odar (1966), Al-Taweel & Carley (1964), Baird *et al.* (1967) and Zimmermann *et al.* (1987). Most of the numerical computations (spherical particles) are restricted to low Reynolds number flows, where approximate theoretical calculations can be made by the methods of singular perturbation expansions [see, for example, Lovalenti & Brady (1993)]. For particles in the intermediate Reynolds number flows, which are most common in engineering applications, it is necessary to solve the complete unstationary Navier–Stokes equations numerically. A numerical computation of this sort is fraught with several problems, e.g. the need for very powerful computers and the lack of appropriate numerical modelling for the free particle motion. The latter problem is synonymous with the well-known problem of grid generation for the simulation of solid body movement in a fluid. The application of data from the calculation of fixed particles with constant or oscillatory local velocities of inflow [see, for example, Mei *et al.* (1991) or Kim *et al.* (1993)] for the case of freely moving particles is rarely possible, since the governing differential equations (Navier–Stokes equations) are only Galilei-invariant. For treatment of this kind of problem, Loehner (1988) suggests a global remeshing approach in combination with an ALE method. After each numerical time step the numerical grid will be examined. If the grid is distorted, a new mesh will be generated. The method of remeshing is, in practice, very complicated

and CPU-time intensive. Other solutions, such as the method described by Raju & Sirignano (1990), enable the motion of particles in one dimension alone.

Overlapping grids have been used in the last 20 years to easily generate meshes for complicated regions [see, for example, Unverdi & Tryggvason (1992), Chesshire & Henshaw (1989) and Benek *et al.* (1985)]. Most of the calculated examples in the above investigations are restricted to the numerical calculation of the Euler equations for fixed rigid bodies.

Here we extend the overlapping grid method for the modelling of freely moving particles in a two-dimensional transient incompressible flow field.

NUMERICAL METHOD

The calculated problems are oriented to the experimental set-up of Schoeneborn with some modifications. A cylindrical particle is located in a rectangular domain. The dimensions of the flow domain are 20×30 particle diameters. The directions of the x- and y-axes and the particle position are shown in figure 1. The gravity force acts in the negative x-axis. The particle is positioned at five particle diameters from the top boundary of the rectangular domain. The outer boundaries of the rectangular grid can be oscillated sinusoidally in the vertical and the horizontal directions. The flow field near the outer boundary will then have the same pulsating velocity.

The equations governing the motion of unsteady, viscous and incompressible flow are the Navier–Stokes equations supplemented by the incompressibility condition. These are:

$$\nabla V = 0$$

$$\frac{\partial V}{\partial t} + (V\nabla)V = -\frac{1}{\rho}\Delta p + v_f \Delta V + F$$

V is the velocity field, ρ and v_f are the density and the kinematic viscosity of the fluid, respectively, P is the pressure and F is the sum of the field forces (here the gravity force).

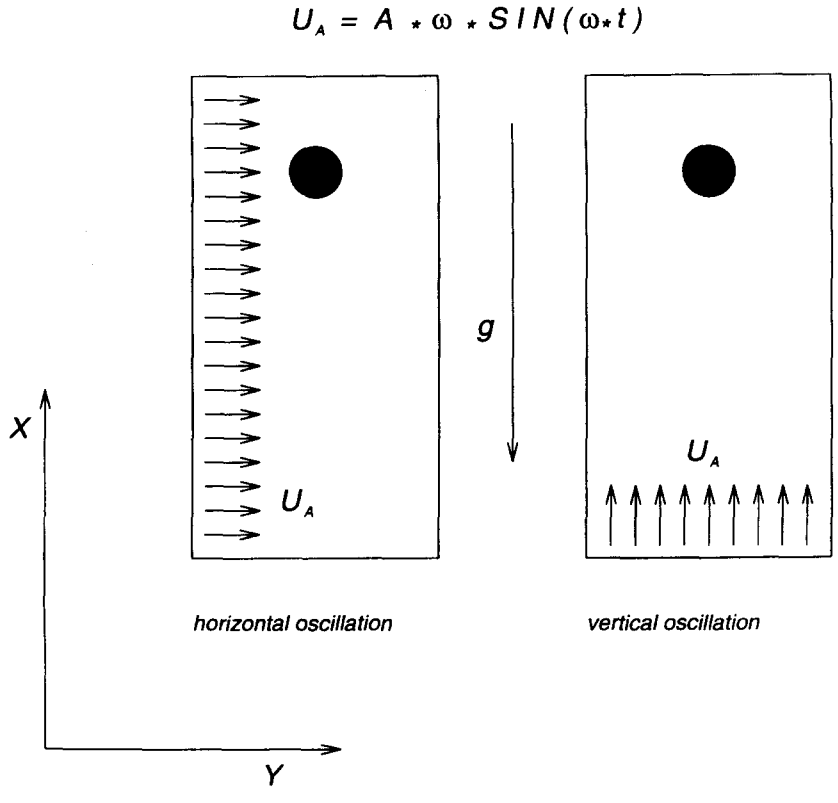

Figure 1. The position of the particle in the rectangular flow domain.

The Navier–Stokes equations are solved numerically with the help of a finite difference method in two different co-ordinate systems. A major Cartesian grid is generated for the whole rectangular flow field. A minor grid is then overset on the major grid so as to resolve the flow around the cylindrical particle without requiring the mesh boundaries to join in any special way. Since the cylindrical particle is an impermeable body, the points of the major grid that fall within the particle (or a curve of the minor grid that circumscribes the particle) are excluded or blanked from the flow field resolution. The boundary of this hole in the major grid becomes the first of two interface boundaries. Data for this hole boundary must be supplied from the solution of the overset cylindrical grid. The outer boundary of the minor grid forms the second interface in this problem and nearby points from the major grid are used to supply flow values along the minor outer boundary. The flow field solutions on each grid are connected by transferring boundary information across these two interfaces.

For the exchange of data between the grids, a bilinear and a biquadratic interpolation are used. The deviation of the results between both interpolation schemes is negligible. The convective terms in the Navier–Stokes equations are discretized with a combination of upwind and central differencing, the viscous terms with the central differencing scheme. For pressure–velocity correction, a checkerboard form and a multigrid form of the SOLA algorithm [see Hirt (1975)] are used. A staggered grid spacing is applied. Special care must be taken in order to account for the realization of various boundary conditions in the staggered grid, e.g. free slip and no slip boundaries with or without vertical and horizontal oscillations. A detailed description defining the various boundary conditions in a staggered mesh can be found, for example, in the work of Kiehm (1986). The boundary conditions applied to the particle surface are the no-slip and, on the outer boundary of the fluid, the free-slip condition with oscillation. The forces and the torque on the particle will be evaluated by integration of the data from the velocity and pressure values on the particle surface; these can easily be obtained from the cylindrical grid. The velocity field of the particulate phase will be described by the kinematic relationships of the rigid body movements. The velocities are scaled with the stationary settling velocity in a fluid at rest, the length scale with the particle diameter, the pressure with the stagnation pressure and the field forces with the Froude number.

The algorithm for the advancement of the numerical solution of the fluid flow and the particle motion in the time domain are as follows:

(1) Generate a rectangular Cartesian grid (major grid) and a cylindrical grid (minor grid) surrounding the particle. Define the position of the particle in the main flow field (major grid).
(2) • The cells of the major grid which are inside the overlapped cylindrical grid (except the cells of the overlapped region) will be marked and blanked.
    • Boundary conditions obtained from the cylindrical grid will be defined on the interface boundaries of the marked and fluid cells of the major grid.
(3) Solve the Navier–Stokes equation in the major Cartesian grid.
(4) Interpolate the boundary conditions on the outer boundary of the cylindrical minor grid from the major grid. Subsequently, solve the Navier–Stokes equations for the cylindrical grid.
(5) Determine the forces and the torque on the particle surface and calculate the velocity of the solid body with the help of the kinematic formulation of a rigid body movement. Move the particle in the major grid. Return to step (2).

The program code is highly vectorized and is carried out on the vector computer at the University of Karlsruhe (SIEMENS-FUJITSU S600). The required CPU-time for each computed case depends on the amplitude and frequency of the fluid oscillation and amounts to several hours.

RESULTS

The following cases are calculated:

- The flow around a fixed cylindrical particle with a constant inflow velocity (no oscillation).
- The flow around a cylindrical particle settling in a bounded fluid at rest (no oscillation).

- The settling motion of a cylindrical particle in a bounded horizontal oscillating fluid.
- The settling motion of a cylindrical particle in a bounded vertical oscillating fluid.

For all cases, the initial velocity of the particle and the fluid field is set at zero.

The first case serves to improve the reliability of the numerical results for various Reynolds numbers. The discrepancies between the calculated drag coefficient C_w of a fixed particle (for a constant inflow velocity, no oscillation) and the experimental data from Schlichting (1982) for various Re numbers are about 3–5%. These discrepancies are due to the two-dimensional calculation of the flow field. Some results of the last two cases will be discussed here. The following velocity plots are presented in a Lagrangian approach (the viewer is located at the particle surface).

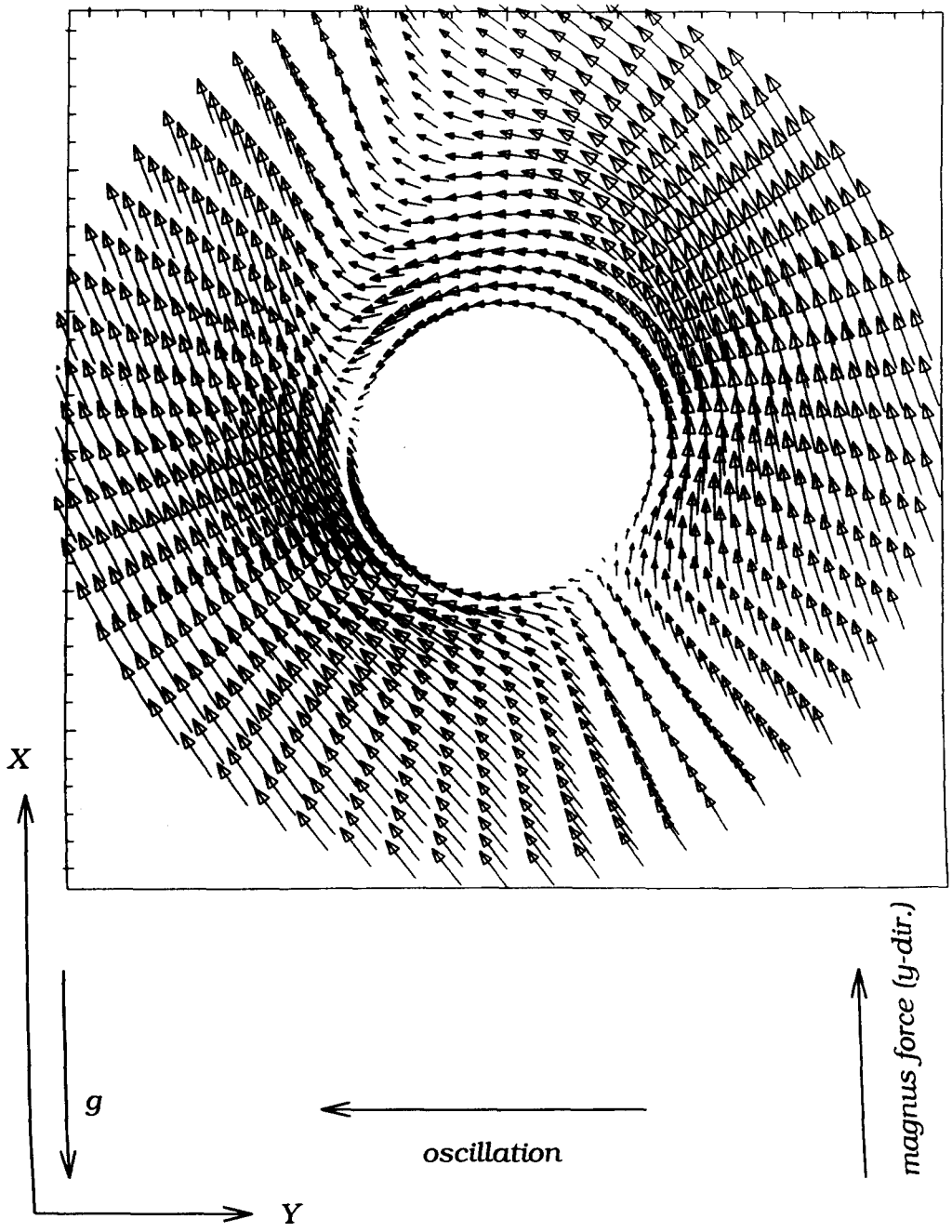

Figure 2. Flow field around the particle for maximal values of the oscillation for $A = 0.1$, $\omega = 10$, $\rho_p/\rho_f = 2.7$ and $\mathrm{Re} = 100$ (negative y-direction).

The horizontal oscillation of the fluid

The settling motion of a particle is followed over 20 time scales. The amplitude of the oscillation is 0.1 particle diameter and the angular frequency is 10. Figures 2, 3 and 4 present the velocity field around the particle for maximal values (in the negative and positive y-direction) and the zero passage of the oscillation. The displacement of the front stagnation point is recognizable. This effect is due to the combined effect of the settling velocity and the additional perpendicular particle velocity caused by the horizontal fluid oscillation. In the wake of the particle another stagnation point develops which depends on the position of the front stagnation point, the elapsed time, the amplitude and the frequency of the oscillatory fluid flow. The flow field in the wake of the particle

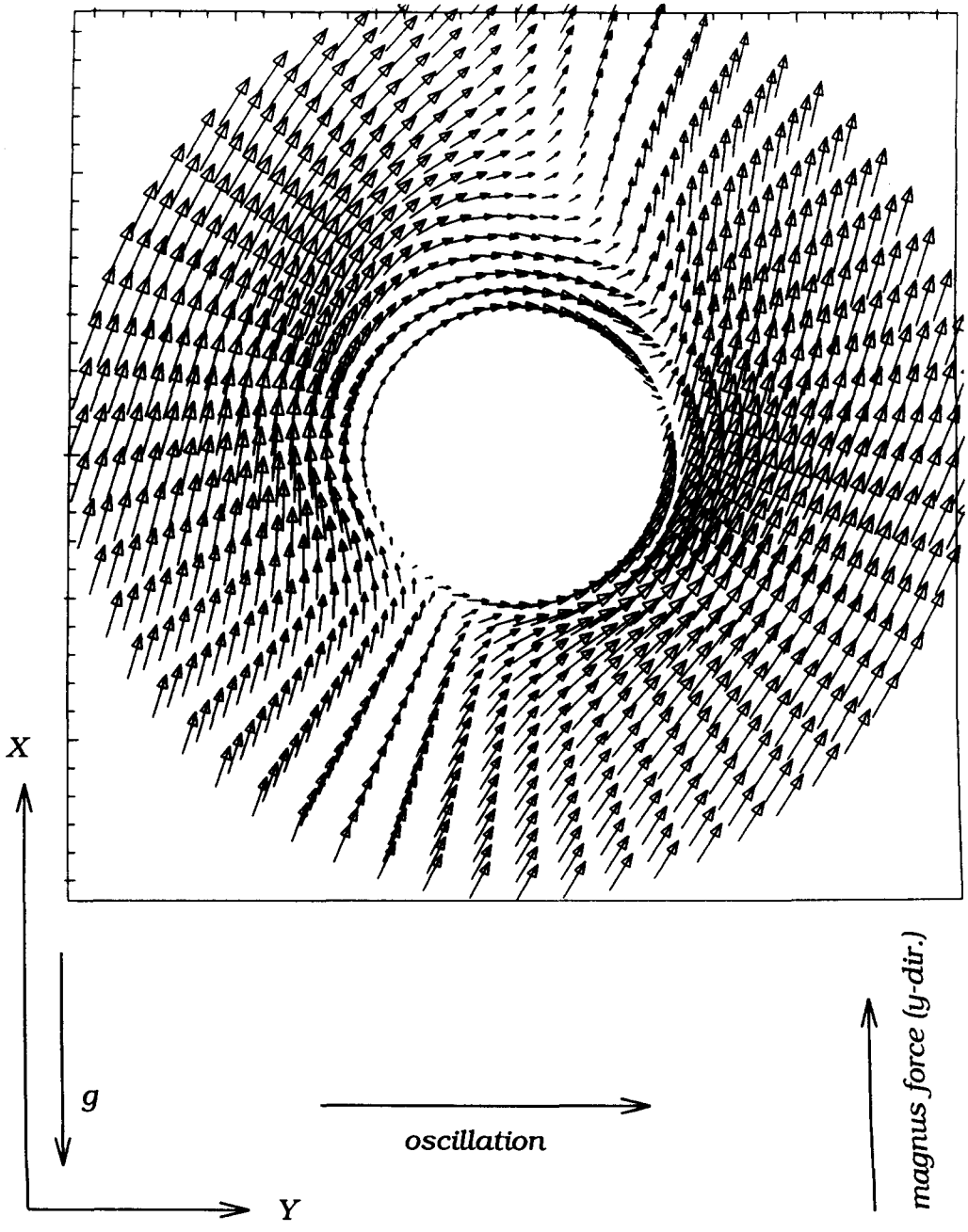

Figure 3. Flow field around the particle for maximum values of the oscillation for $A = 0.1$, $\omega = 10$, $\rho_p/\rho_f = 2.7$ and $\mathrm{Re} = 100$ (positive y-direction).

is highly affected by the oscillatory horizontal fluid flow, which prevents vortex shedding in the wake of the particle except for the case where the oscillation has nearly zero passage (figure 4). The circulatory flow around the particle causes additional buoyancy (magnus) forces on the particle (see figures 2 and 3).

The vertical oscillation of the fluid

Experimental works concerning this problem are mentioned above. A strict comparison of the experimental data to the numerical calculations of the present investigation is, due to the discrepancies between the flow around cylindrical and spherical bodies, not possible. The settling motion of a particle in an oscillatory flow field is influenced by the following parameters:

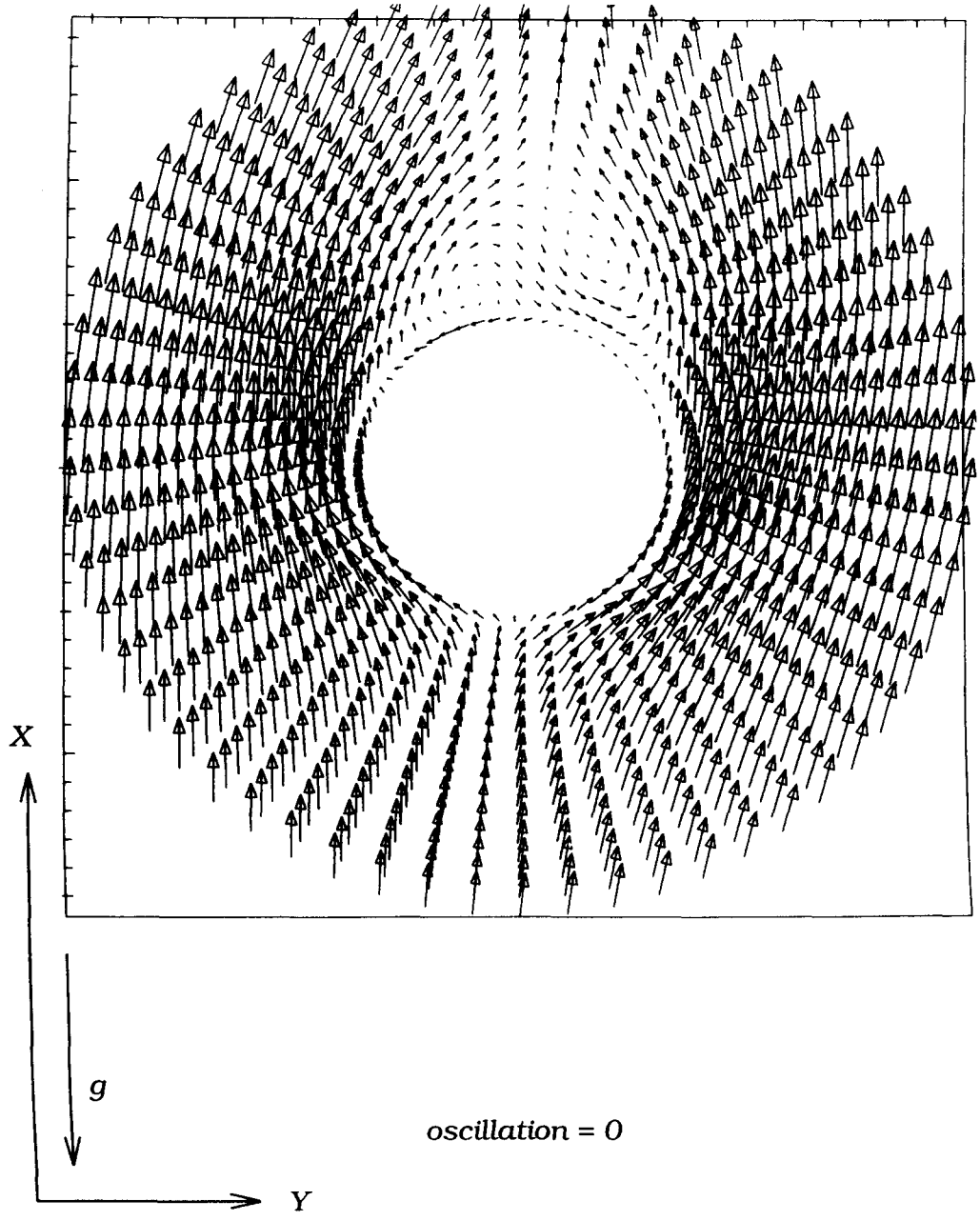

Figure 4. Flow field around the particle for the zero passage of the oscillation for $A = 0.1$, $\omega = 10$, $\rho_p/\rho_f = 2.7$ and $\mathrm{Re} = 100$.

Table 1. Computed cases

Reynolds number Re	Density ratio ρ_p/ρ_f	Amplitude A	Angular frequency ω
100	1.5	0.1–0.6	10
100	1.5	0.5	2–13
100	2.7	0.1–0.6	10
100	2.7	0.5	2–13
300	2.7	0.1–0.6	10
300	2.7	0.5	2–13

(a) Reynolds number Re, (b) the density ratio between the particle and the fluid ρ_p/ρ_f, and (c) the angular frequency ω and amplitude A of the oscillation. The variation of the angular frequency and amplitude takes place in the range of 0–13 and 0.1–0.6 particle diameters. The Reynolds numbers have values of 100 and 300, the values of the density ratios are $\rho_p/\rho_p = 1.5$ (synthetic material particles in water) and 2.7 (glass particles in water). Table 1 gives an overview of the computed cases.

Figures 5 and 6 present the velocity field surrounding the particle (cylindrical grid) shortly after the settling motion of the particle. As seen in the vector plots, the oscillation alternates with and against the direction of the settling velocity. The velocities in the plots are scaled with the maximal velocity V_{max} of the flow field. The velocity field in the lower and upper half of the presented flow domain is fully symmetrical.

Figures 7 and 8 show the velocity field of more than nine time scales. In the case where the oscillatory flow is in the direction of the settling velocity, a relatively strong flow can be recognized in the particle wake. The velocity field for these cases is likewise approximately symmetrical.

Phase lag. The phase lag for all the computed cases is small. Figure 9 demonstrates the comparison of the particle velocity with the fluid velocity for Re = 100, $\rho_p/\rho_f = 1.5$, $A = 0.5$ and $\omega = 5$. According to the experimental investigations of Al-Taweel & Carley a noticeable phase lag can be expected at higher density ratios ($\rho_p/\rho_f \geqslant 10$).

Forces. The maximal values of the forces on the particle (oscillatory part) are correlated with the maximal values of the fluid acceleration $A \cdot \omega^2$ (see figure 10). The relationship is linear and is a function of the density ratio. The maximal forces are nearly identical for the density ratio $\rho_p/\rho_f = 2.7$ and the Reynolds numbers Re = 100 and 300.

Amplitude ratio. The amplitude ratio is characteristic of the particle–fluid interaction. It is defined as:

$$\frac{A_f}{A_p} = \frac{\text{amplitude of the fluid oscillation}}{\text{amplitude of the particle oscillation}}$$

Figures 11 and 12 present the amplitude ratio versus the variation of the frequency and the amplitude of the fluid oscillation. The amplitude ratio decreases with the increase of fluid frequency and density ratio (the influence of the flow field on the particle motion decreases). It tends to a constant value at high frequencies. Compared to the density ratio, the influence of Reynolds number on the amplitude ratio is negligible.

The behaviour of the amplitude ratio versus the amplitude of the fluid oscillation is nearly constant. This means that variation of the chosen amplitude has no substantial effect on the amplitude ratio (the fluid–particle interaction). The influences of the Reynolds number and the density ratio on the amplitude ratio are nearly the same as in the case of frequency variation.

Retarding effect. The ratio of the average fall velocity in an oscillating flow field to the fall velocity in a fluid at rest is called the retarding effect. It is defined as:

$$\frac{V_s^*}{V_s} = \frac{\text{average settling velocity in an oscillating flow field}}{\text{average settling velocity in a fluid at rest}}$$

Figures 13 and 14 demonstrate the retarding effect versus the frequency and amplitude of the oscillation. The retarding effect increases with the increase of frequency and amplitude of the fluid oscillation. The retarding effect increases with the increase of the density ratio and the decrease of the Reynolds number.

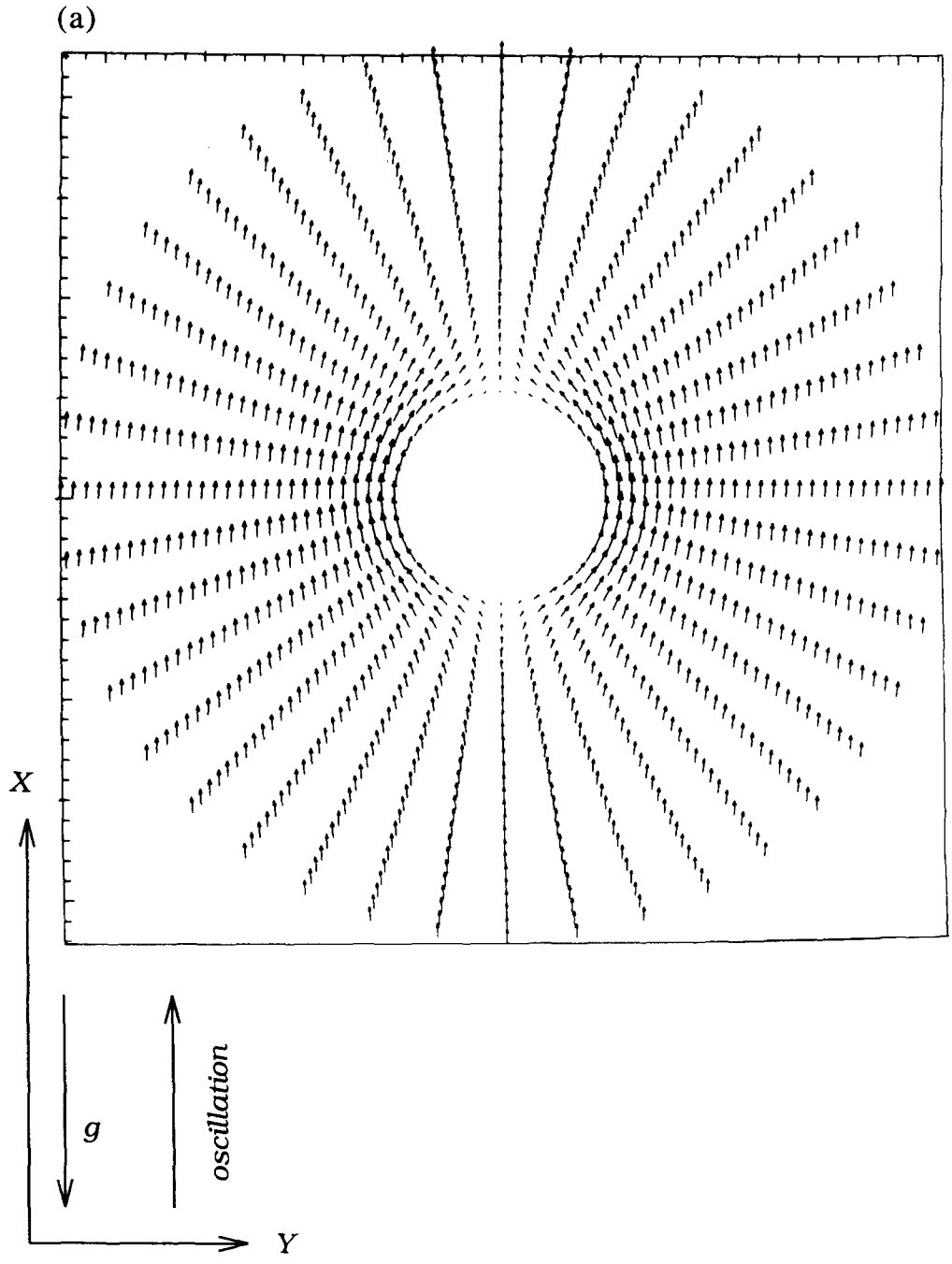

Fig. 5(a). *Caption opposite.*

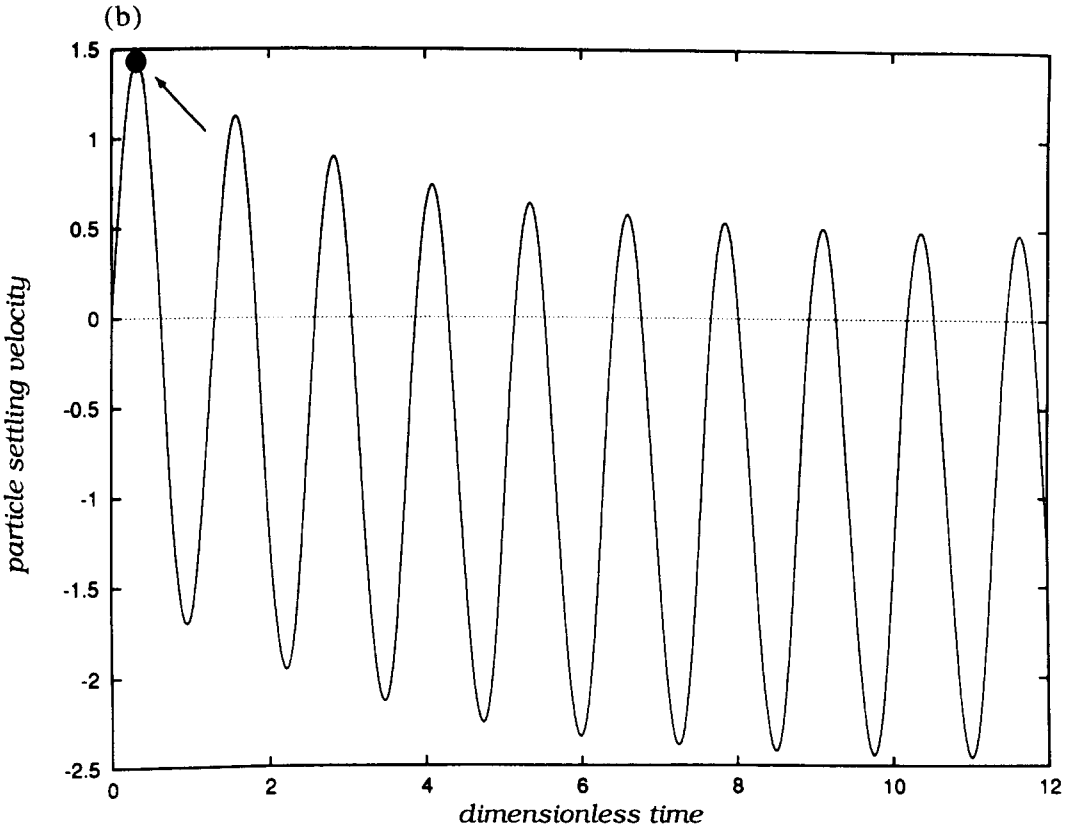

Fig. 5(b)

Figure 5. (a) Flow field around the particle for the case that the oscillation is against the particle settling direction for $A = 0.5$, $\omega = 5$, $\rho_p/\rho_f = 1.5$, $t = 0.31$, Re = 100 and $V_{max} = 1.678$. (b) Particle settling velocity vs time for (a).

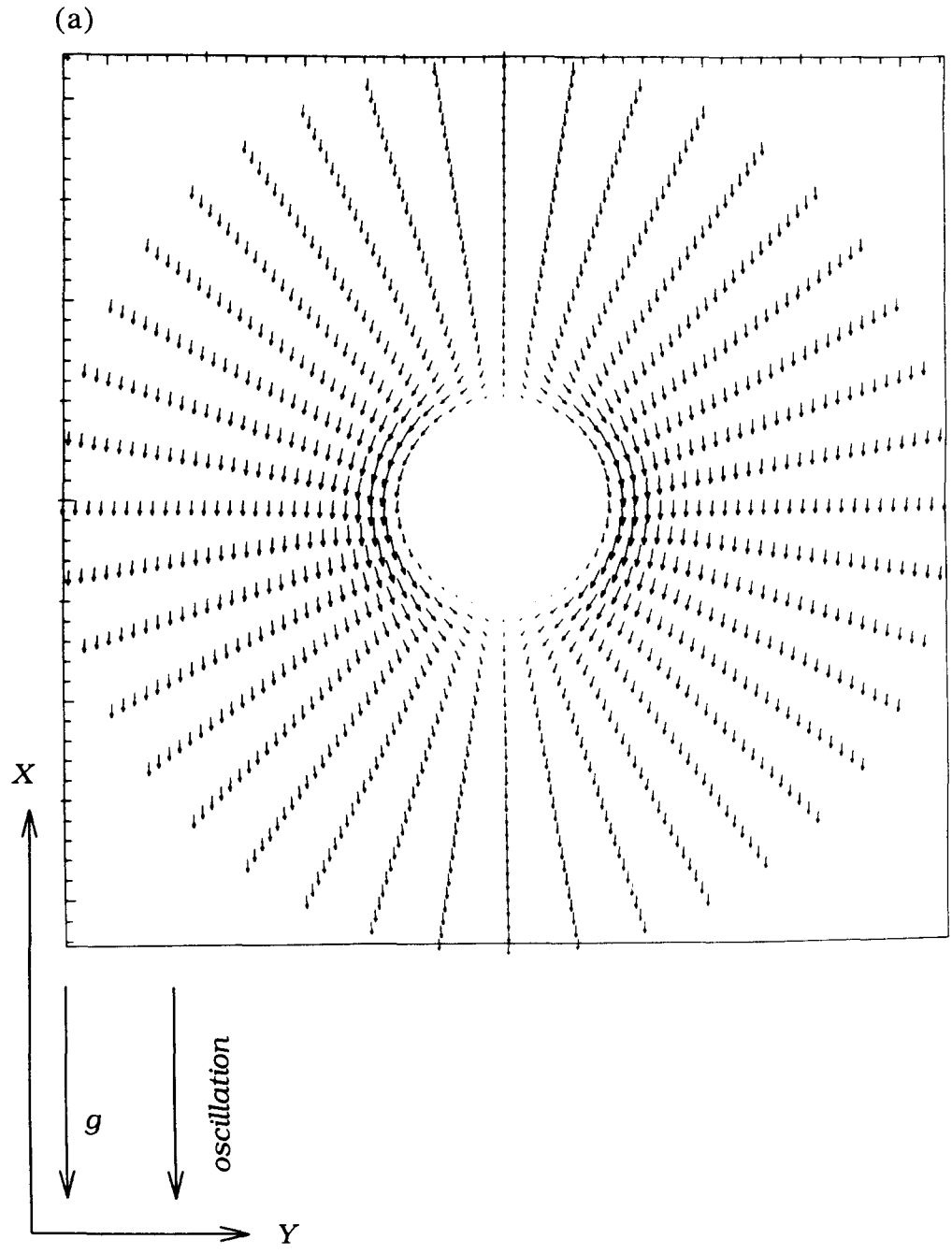

Fig. 6(a). *Caption opposite.*

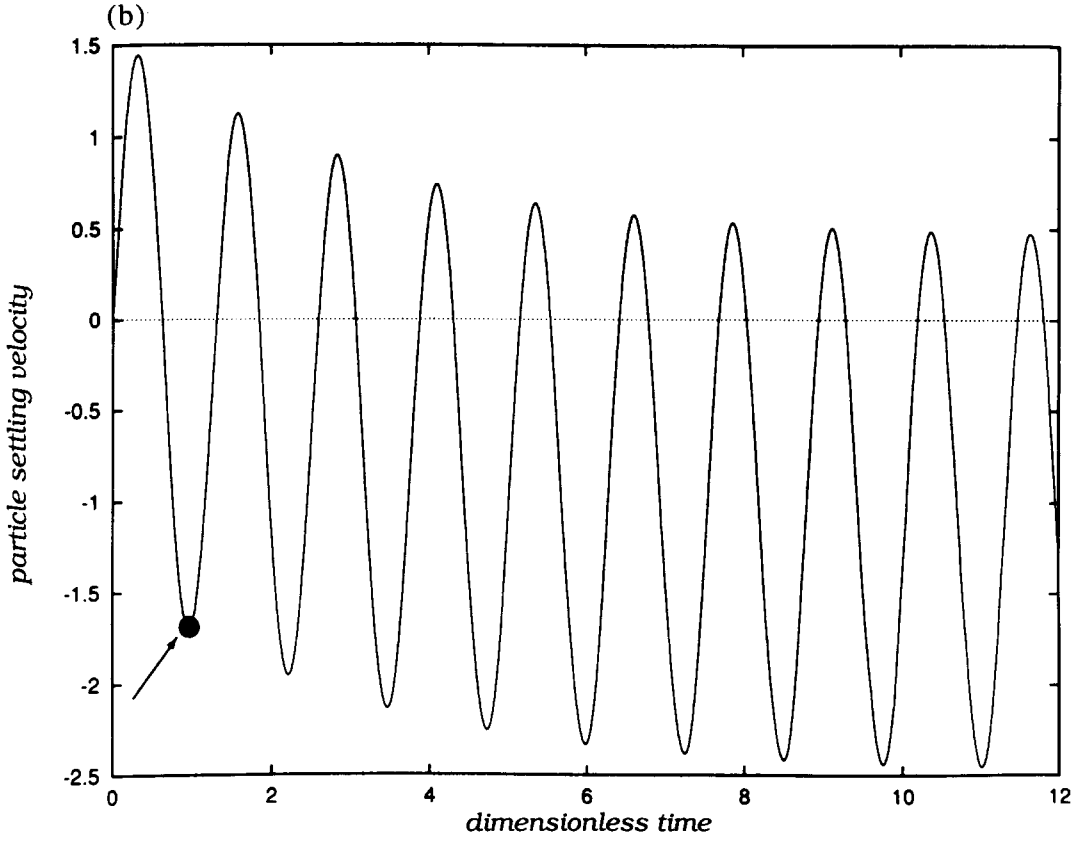

Fig. 6(b)

Figure 6. (a) Flow field around the particle for the case that the oscillation is in the particle settling direction for $A = 0.5$, $\omega = 5$, $\rho_p/\rho_f = 1.5$, $t = 0.96$, Re = 100 and $V_{max} = 1.57$. (b) Particle settling velocity vs time for (a).

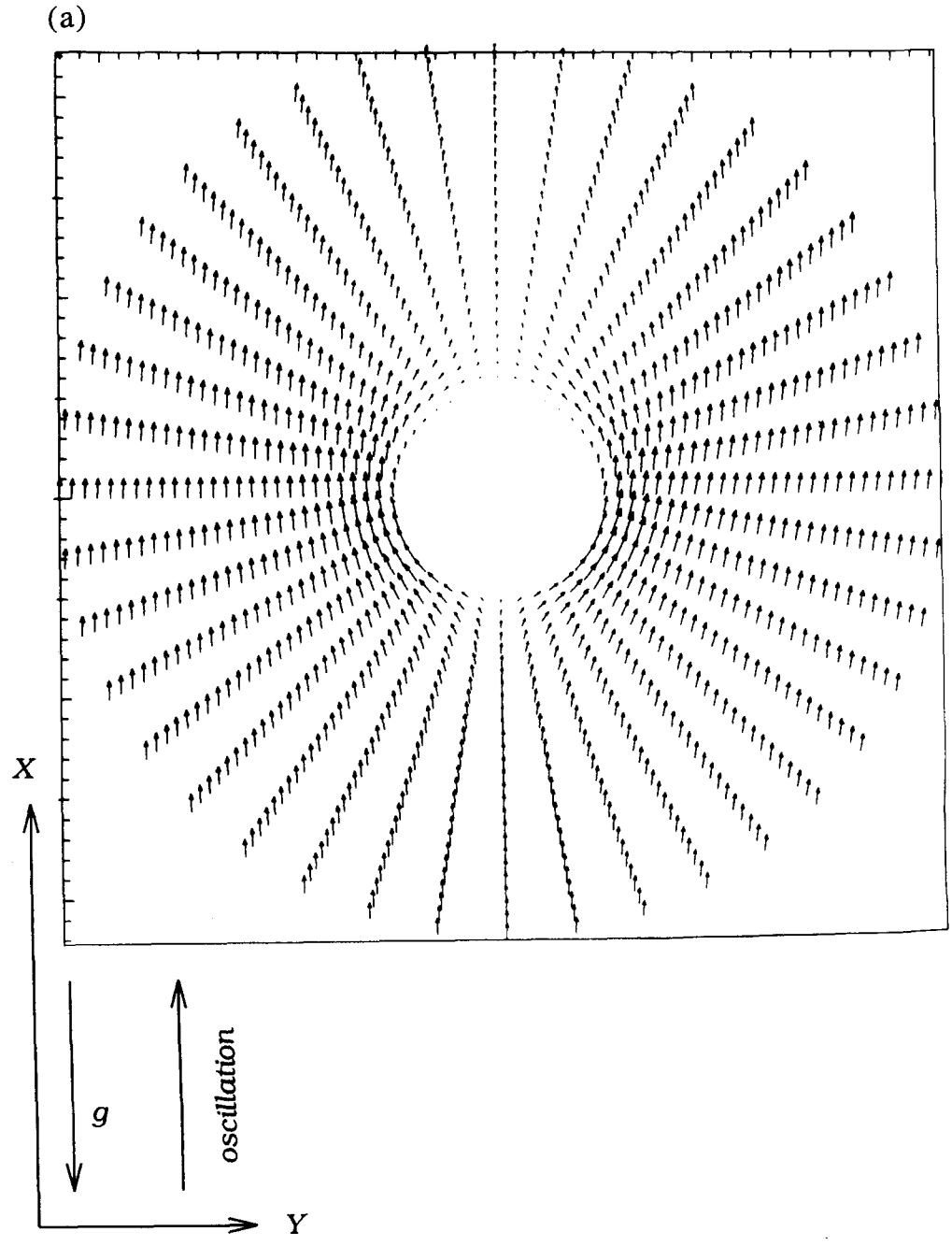

Fig. 7(a). *Caption opposite.*

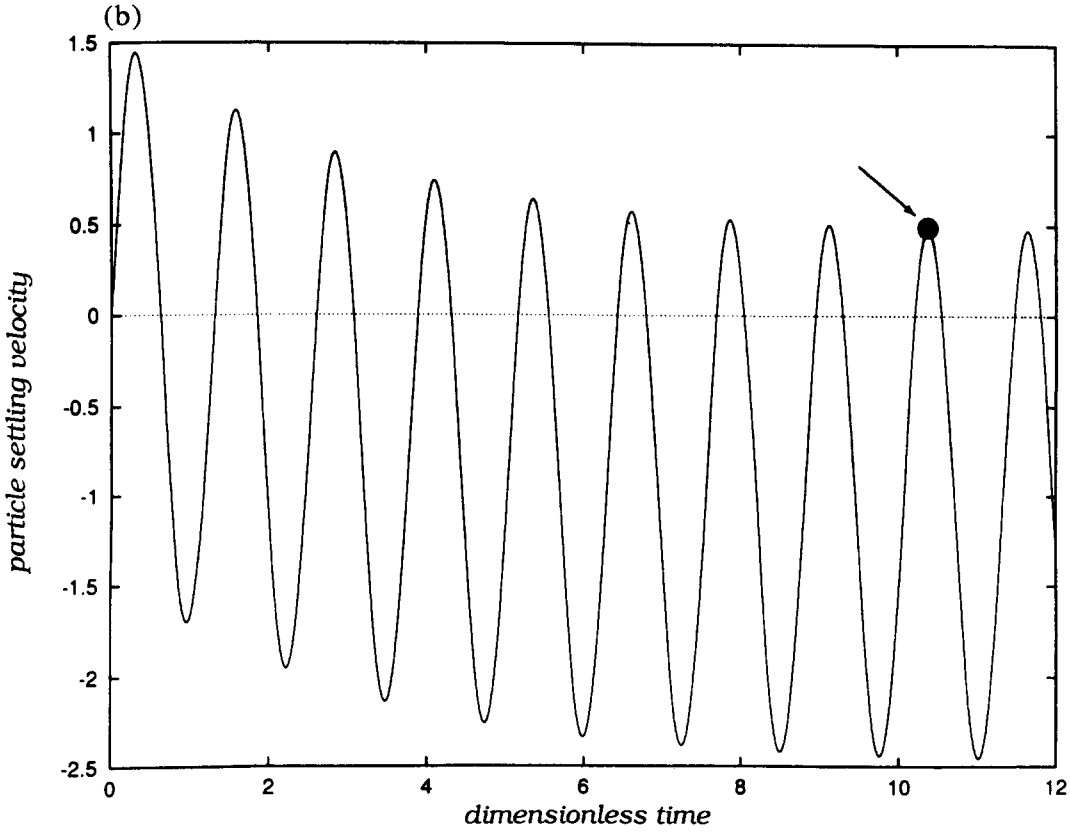

Fig. 7 (b)

Figure 7. Flow field around the particle for the case that the oscillation is against the particle settling direction for $A = 0.5$, $\omega = 5$, $\rho_p/\rho_f = 1.5$, $t = 10.38$, Re = 100 and $V_{max} = 2.83$. (b) Particle settling velocity vs time for (a).

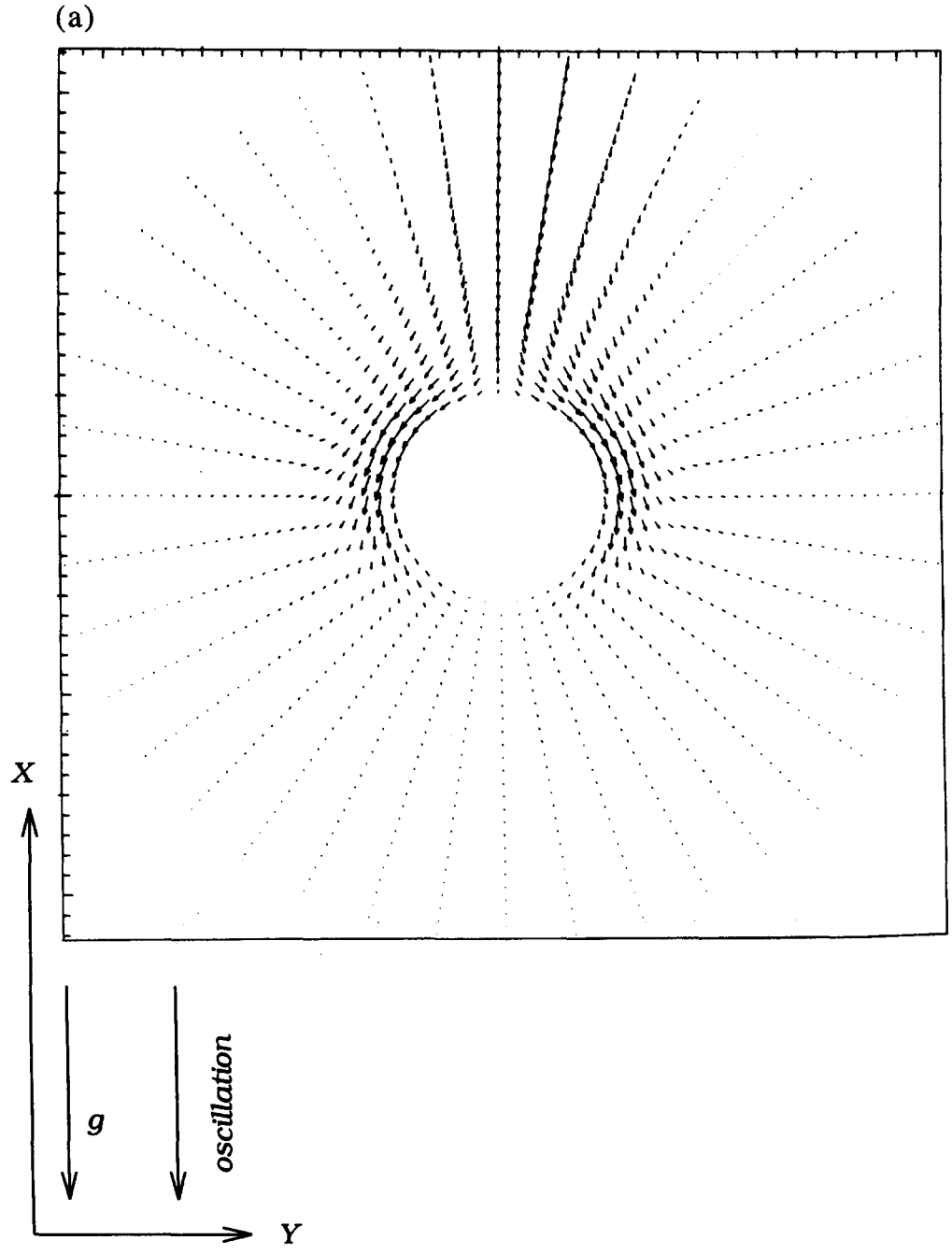

Fig. 8(a). *Caption opposite.*

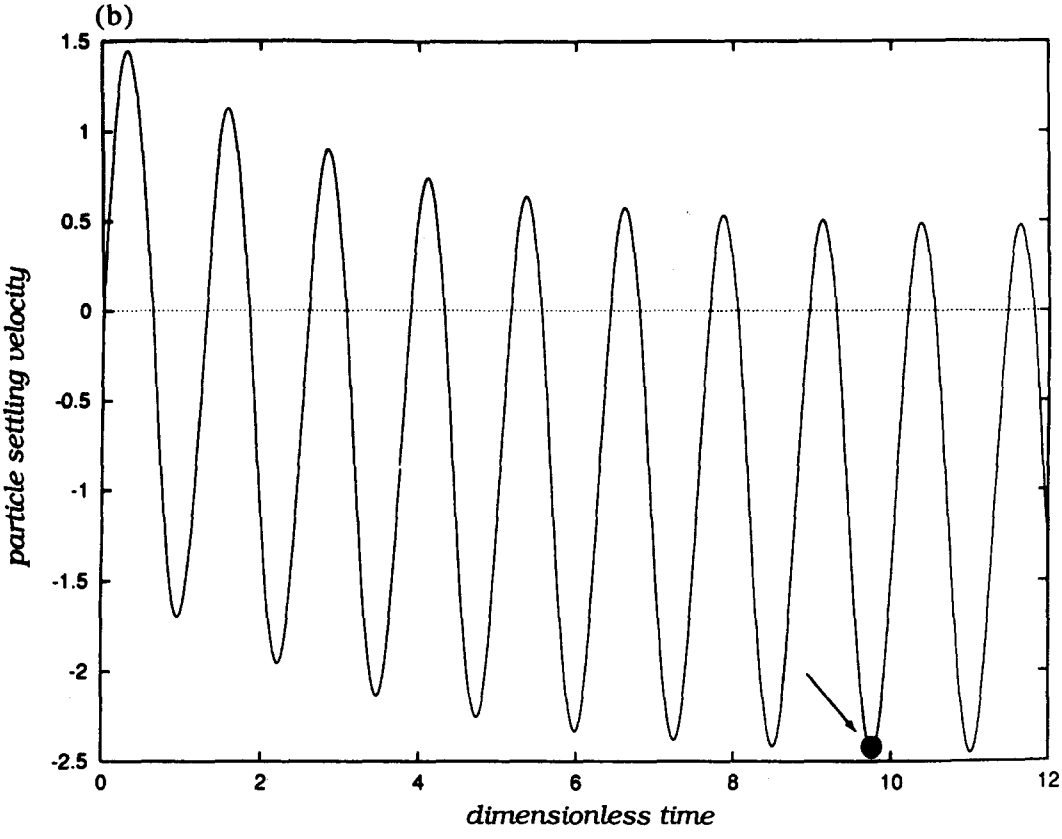

Fig. 8(b)

Figure 8. (a) Flow field around the particle for the case that the oscillation is in the particle settling direction for $A = 0.5$, $\omega = 5$, $\rho_p/\rho_f = 1.5$, $t = 9.77$, Re = 100 and $V_{max} = 1.55$. (b) Particle settling velocity vs time for (a).

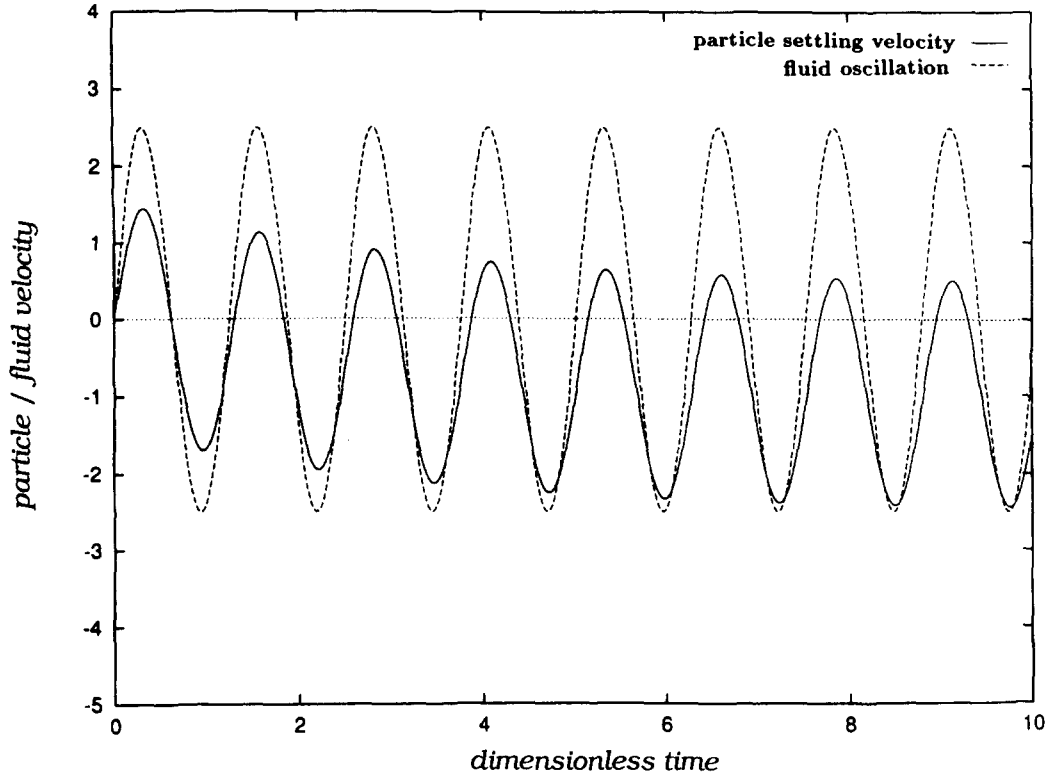

Figure 9. Comparison of a particle–fluid velocity for $A = 0.5$, $\omega = 5$, $\rho_p/\rho_f = 1.5$ and $\mathrm{Re} = 100$.

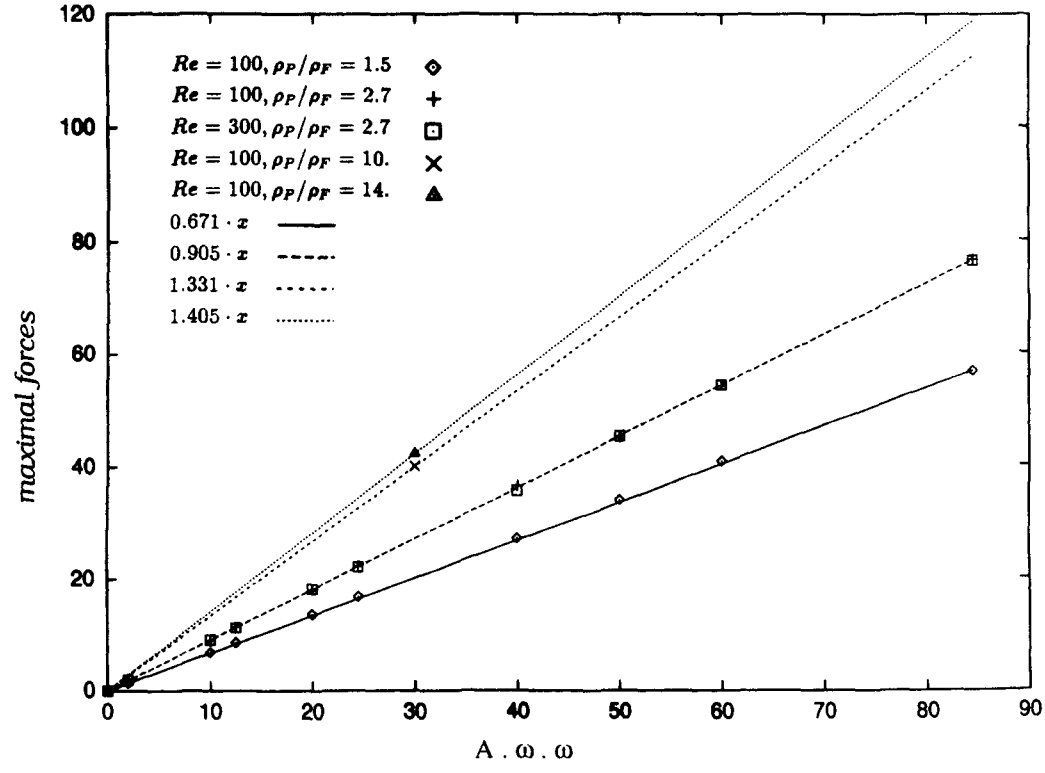

Figure 10. Correlation of the maximum values of forces with $A\omega^2$.

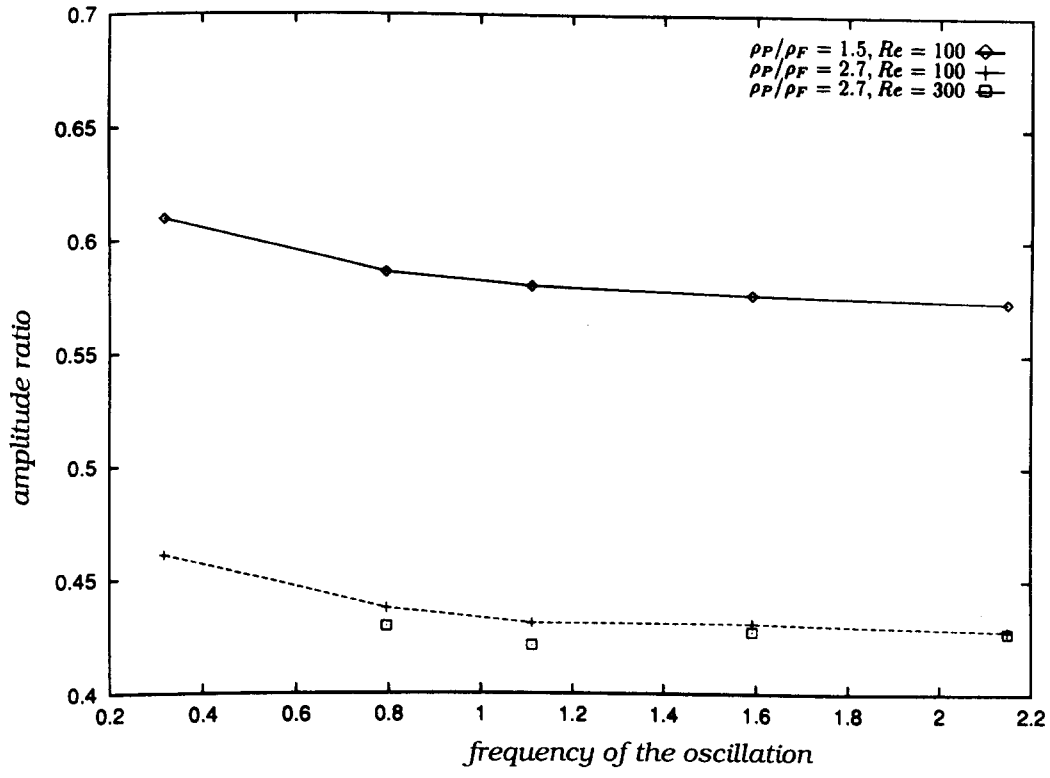

Figure 11. Amplitude ratio vs the variation of the frequency for $A = 0.5$.

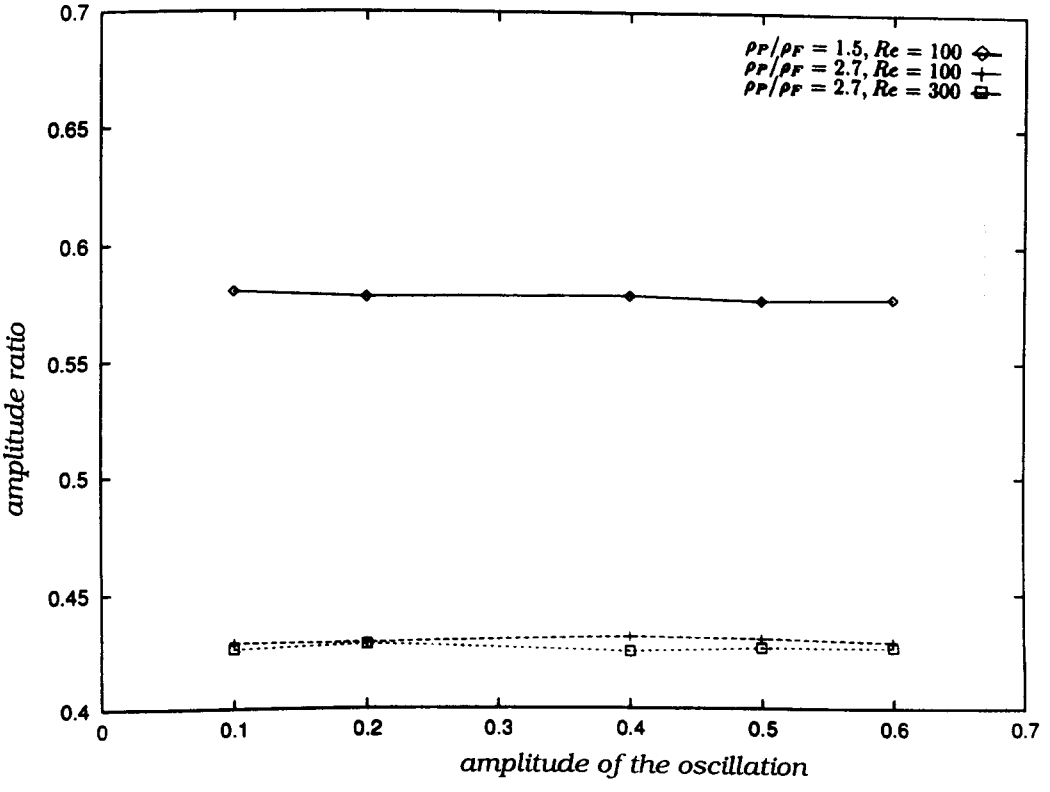

Figure 12. Amplitude ratio vs the variation of the amplitude for $\omega = 10$.

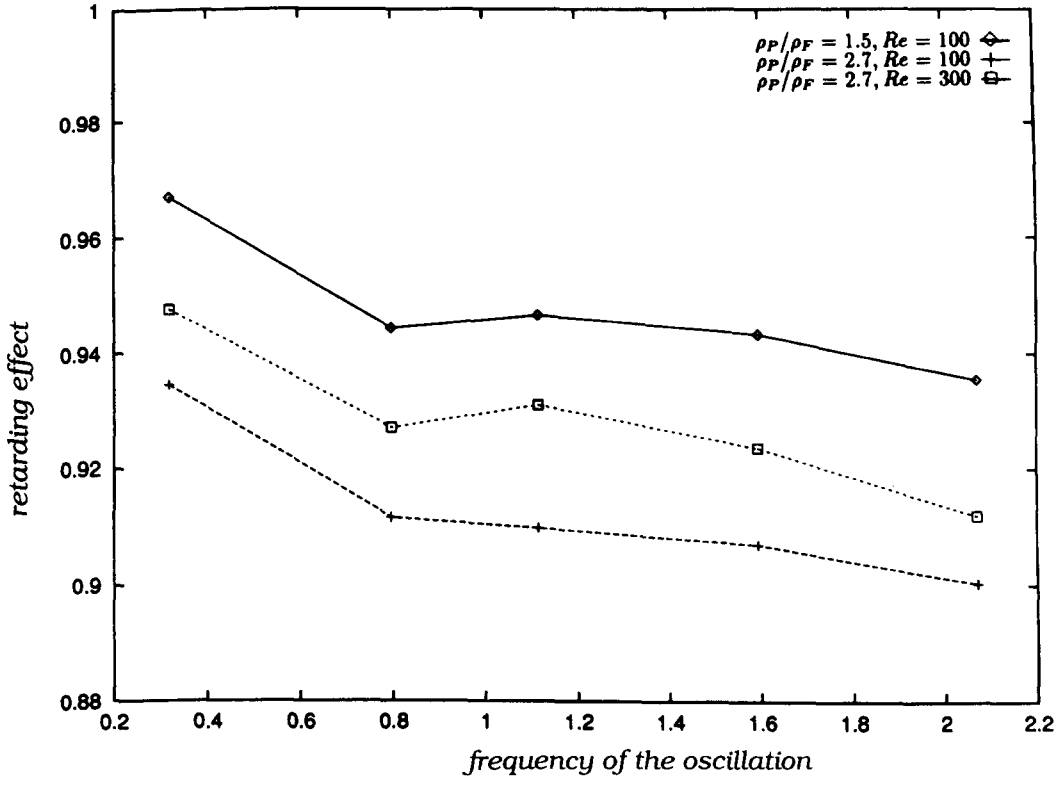

Figure 13. Retarding effect vs the variation of the frequency for $A = 0.5$.

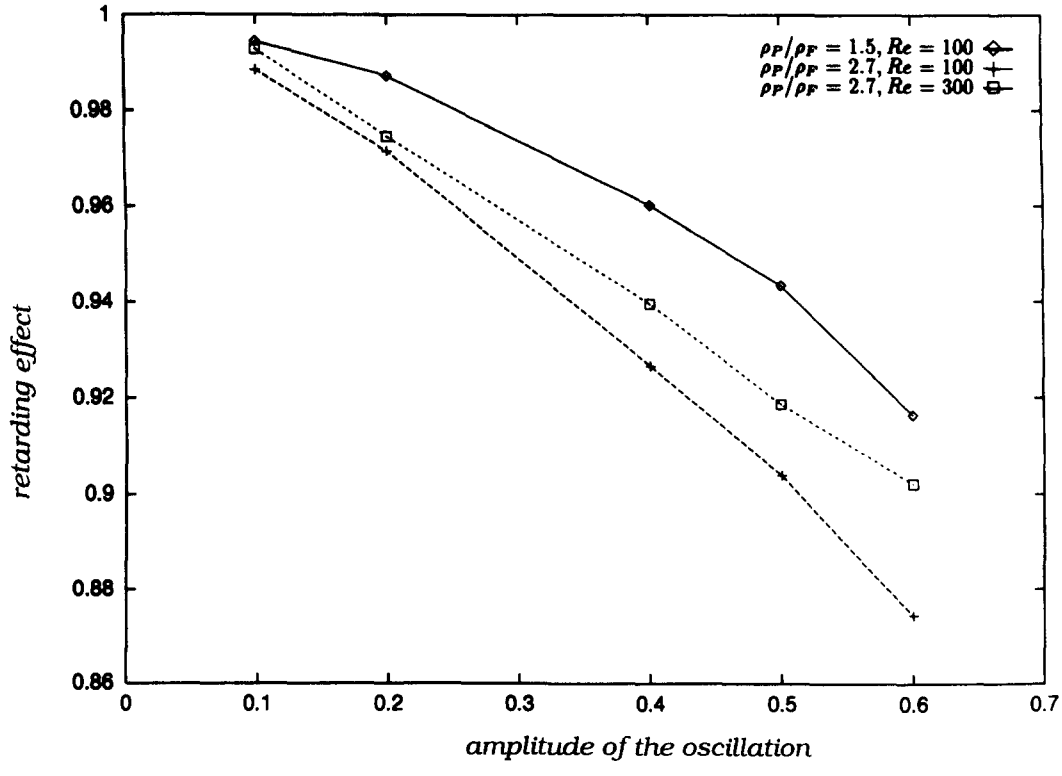

Figure 14. Retarding effect vs the variation of the amplitude for $\omega = 10$.

CONCLUSIONS

The method of overlapping grids can be easily applied to the problem of particle motion in an unsteady flow field. Several types of problems can be solved with this grid approach. Numerical computations of a cylindrical particle motion in a sinusoidally horizontally and vertically oscillating flow were performed. In both cases the flow around the particle is distinguished from the flow around a fixed particle. These differences essentially appear in the wake of the particle. For horizontal oscillation of the flow field the front stagnation point is displaced. A second stagnation point is developed in the particle wake. The influences of Reynolds number and density ratio on the forces (on the particle), the amplitude ratio and the retarding effect have been investigated with regard to the vertical oscillation of the flow field. There is a weak influence of the Reynolds number on the forces and the amplitude ratio. The influence of density ratio is dominant. Further work must be carried out for the three-dimensional numerical simulation of spherical particles in unsteady oscillatory flows.

REFERENCES

AL-TAWEEL, A. M. & CARLEY, J. 1964 Dynamics of a single sphere in pulsated flowing liquids: Part I experimental method and result. *AIChE Symp. Ser.* **67,** 114–123.

BAIRD, M. H. I., SENIOR, M. G. & THOMPSON, R. J. 1967 Terminal velocities of spherical particles in a vertically oscillating fluid. *Chem. Engng Sci.* **22,** 551–558.

BENEK, J. A., STEGER, J. L. & DOUGHERTY, F. C. 1985 On application of chimera grid schemes to store separation. NASA-TM-88193.

CHESSHIRE, G. & HENSHAW, W. D. 1989 Composite overlapping meshes for the solution of partial diffrential equations. *J. Comput. Phys.* 1–65.

HIRT, W. C., NICHOLS, B. D. & ROMERO, N. C. 1975 SOLA—a numerical solution algorithm for transient fluid flows. Los Alamos Scientific Laboratory, New Mexico, LA-5842.

KIEHM, P. 1986 Numerische Untersuchungen der laminaren Stroemungsfelder und des Waerm-euebergangs in einem Kanal mit quereingebautem Kreiszylinder. Ph.D. thesis at the University of Bochum, Germany.

KIM, J., ELGHOBASHI, S. & SIRIGNANO, A. W. 1993 Three dimensional flow over two spheres placed side by side. *J. Fluid Mech.* **246,** 465–488.

LOEHNER, R. 1988 An adaptive finite-element-solver for transient problems with moving bodies. *Comput. Struct.* **30,** 303–317.

LOVALENTI, P. M. & BRADY, J. F. 1993 The force on a sphere in a uniform flow with small-amplitude oscillations at finite Reynolds number. *J. Fluid Mech.* **256,** 607–614.

MEI, R., CHRISTOPHER, J. L. & ADRIAN, R. 1991 Unsteady drag on a sphere at finite Reynolds number with small fluctuation in the free stream velocity. *J. Fluid Mech.* **223,** 613–631.

ODAR, F. 1966 Verification of the proposed equation for calculation of the forces on a sphere accelerating in a viscous fluid. U.S.A. Cold Regions Research and Engineering Laboratory Research Report 190.

ODAR, F. & HAMILTON, W. J. 1964 Forces on a sphere accelerating in a viscous fluid. *J. Fluid Mech.* **18,** 302–314.

RAJU, M. S. & SIRIGNANO, W. A. 1990 Interaction between two vaporizing droplets in an intermediate Reynolds number flow. *Phys. Fluids A* **2,** 1780–1795.

SCHLICHTING, H. 1982 *Grenzschicht-Theorie.* Braun, Karlsruhe, Germany.

SCHOENEBORN, P. R. 1975 The interaction between a single particle and an oscillating fluid. *Int. J. Multiphase Flow* **2,** 307–317.

UNVERDI, S. O. & TRYGGVASON, G. 1992 A front-tracking method for viscous, incompressible, multi-fluid flows. *J. Comp. Phys.* **100,** 25–37.

WILLEKE, K. W. & BARON, P. B. 1992 *Aerosol Measurement, Principles Techniques and Applications,* p. 563. Van Nostrand, New York.

ZIMMERMANN, M., SCRIVENER, O., ANDRIEU, J. P. & FEIDT, R. 1987 Trennung von Feststoff/Wasser-Gemischen bei pulsierender Stroemung. *Chem. Ing. Technol.* **59,** 216–218.